Eldrid Charles (Orcid ID: 0000-0001-5306-3644)

Concentration-Dependent Coulombic Effects in TWIMS CCS Calibration

Charles Eldrid[1,†], Eloise O'Connor[1,†], Konstantinos Thalassinos[1,2,]*

[1]Institute of Structural and Molecular Biology, University College London, Gower Street, London WC1E 6BT, UK

[2]Institute of Structural and Molecular Biology, Birkbeck University, Malet Place, London WC1E 7HX, UK

[†]Authors contributed equally to work,

**Corresponding author k.thalassinos@ucl.ac.uk*

This article has been accepted for publication and undergone full peer review but has not been through the copyediting, typesetting, pagination and proofreading process which may lead to differences between this version and the Version of Record. Please cite this article as doi: 10.1002/rcm.8613

Abstract

Rationale: Travelling wave ion mobility spectrometry (TWIMS) is increasingly being used as a method for calculating the collision cross section (CCS) of protein ions. To calculate the CCS of unknown ions, however, the TWIMS device needs to be calibrated using calibrant proteins of known CCS values. The effect of calibrant protein concentration of the accuracy of the resulting calibration curve has not been explicitly studied so far. We hypothesised that at high protein concentrations the ion density within the TWIMS device will be such that ions will experience *space charge effects* resulting in deviations, as well as broadening, of ion arrival time distributions (ATDs). Calibration curves using these altered ATDs would therefore result in incorrect CCS values being calculated for the protein ions of interest.

Methods: Three protein CCS calibrants, avidin, bovine serum albumin and β-lactgobulin, were prepared at different concentrations and used to calculate the CCS of a non-calibrant protein. Data were collected on a Synapt G1 ion mobility-mass spectrometer with a nano-electrospray ionisation (nESI) source using capillaries prepared *in house*.

Results: Increasing the concentration of CCS calibrants caused ATD broadening and shifted the ATD peak tops, leading to a significant increase in calculated CCS values.

Conclusion: The concentration of protein calibrants can directly affect the quality of the CCS calibration in TWIMS experiments.

Introduction

Native mass spectrometry as a field has expanded since the invention of electrospray and MALDI ionisation,[1–3] and it can provide important information on protein behaviour, protein-protein and protein-ligand interactions.[4,5] Ion mobility (IM) spectrometry allows the separation of ions based on their reduced mobility (K_0) through a gas, from which their collision cross section (CCS), or more accurately their momentum transfer cross section[6], can be calculated via the measurement of several variables. The CCS is a parameter which can be used to calculate differences of ion structure in terms of nm^2 or $Å^2$. When combined with native mass-spectrometry, ion mobility can give important information regarding protein behaviour, conformation, stability and domain organisation.[7–15] In IM spectrometry ions travel through an inert drift-gas, such as helium or nitrogen, and undergo collisions with the neutral gas molecules. Larger or more extended ions will undergo a greater number of collisions with the drift-gas, and so travel through the drift-cell more slowly than an ion which is more compact. This allows separation of isobaric ions based on conformation. In drift-tube IM the CCS of ions can be directly calculated from the time that they take to traverse the drift-cell, or the arrival time distribution (ATD), using the Mason-Schamp equation:

$$\Omega = \frac{3ez}{16N}\left(\frac{2\pi}{\mu k_B T}\right)^{\frac{1}{2}}\frac{1}{K_0}$$

The CCS (Ω) and the drift-mobility (K_0) are inversely proportional and can be calculated with knowledge of parameters such as the ionic charge (z), drift gas density (N), reduced mass of the colliding ion (μ) and absolute temperature in Kelvin (T). e and k_B represent elementary charge and the Botlzmann constant, respectively.[16] The relationship between the CCS and the K_0 of an ion is inversely proportional at the 'low field limit' or below.[17] Travelling wave ion mobility spectrometry (TWIMS) uses DC pulses through stacked ring ion guides to create an electrical wave, which carries ions through the IM cell, and is present in quadrupole time-of-flight (QToF) instruments, such as the Synapt.[18–20] While TWIMS helps balance separation without loss of sensitivity through radial confinement[18], the mobility of ions through the buffer gas is complex due to the non-uniform and time dependent electric field, and therefore the Mason-Schamp equation is not applicable.

TWIMS instruments can be modified in order to calculate the CCS directly, without use of the Mason-Schamp equation, as shown by Giles *et al*[21] with a modified Synapt instrument. An ion with a CCS allowing it to ride directly on the peak of a wave would have a specific mobility which matched the speed of the wave travelling through the TWIMS IM cell; however, multiple modifications had to be made in order to achieve this. The apertures at the entrance and exit of the TWIMS drift-cell were reduced in order to allow increased pressure in the drift region, the pressure gauges were upgraded to allow more accurate measurements, and the T-wave electronics were overhauled to allow more accurate control of the T-wave parameters. Another method of direct CCS calculation was presented by Mortensen *et al*, which models the motion of the waves themselves but requires the use of low wave velocities; otherwise, the CCS values differ considerably from the reported values.[22] In the majority of cases, however, biomolecules of known CCS value are used as calibrants.

Through the use of CCS calibrants,[23–31] the CCS values of unknown biomolecules can be calculated from arrival times. Three different methods are commonly described, presented by Ruotolo *et al*,[32] Smith *et al*,[33] and Thalassinos *et al* [34]. The Ruotolo *et al*, and Thalassinos *et al*, methods do not differ significantly as they both calculate the mass-corrected drift-time for calibrants by subtracting the time spent in the mobility and ToF regions by ions, based on the T-wave velocity and the *m/z* value and charge of the ion. The Smith *et al* method considers this time to be negligible and thus does not calculate it. All three methods require the calculation of the corrected CCS (Ω') using the reduced mass and charge of the ion in questions. Only the Thalassinos *et al*[34] method – which is used in this paper – will be described in detail.

First, the effective drift-time, $t(d)'$, is calculated by subtracting the offset time (t_o) from the drift-time ($t(d)$) that the ions spend in the transfer and mobility regions which is related to the T-wave velocity. At a velocity of 300 ms^{-1} the time per plate is 0.01 s; therefore, the time per plate in the mobility (t_m) and transfer region (t_t) at T-wave velocity *v* is:

$$t_m = \frac{0.01 \times 300}{v_m} \text{ and } t_t = \frac{0.01 \times 300}{v_t}$$

The time-per-plate in both regions is then multiplied by the number of stacking-ring ion guide (SRIG) plates, which is 61 and 31, respectively, in a Synapt G1 instrument.

$$t_o = (t_m \times 61) + (t_t \times 31)$$

The $t(d)'$ is then corrected for the mass-dependent flight time, which is 0.085 msec for an ion of *m/z* 1000 in a Synapt G1:

$$t(d)'' = t(d)' - \sqrt{\frac{m/z}{1000}} \times 0.085$$

The collision cross-section (Ω) must be corrected for mass (Ω'), where m_i is the mass of the calibrant, m_n is the mass of the buffer gas, and z is the charge of the ion:

$$\Omega' = \frac{\Omega}{z\left(\frac{1}{m_n} - \frac{1}{m_i}\right)^{\frac{1}{2}}}$$

To create a calibration curve Ω' is plotted against $t(d)''$, and the Ω' of an unknown ion can be calculated using:

$$\Omega' = (t(d)'')^N \times A \times z\left(\frac{1}{m_n} - \frac{1}{m_i}\right)^{\frac{1}{2}}$$

where N and A are parameters calculated from a line of power fit which has the equation $y = Ax^N$, z is the charge of the ion, m_i is the mass of the ion and m_n is the mass of the buffer gas. The process of CCS calibration using the Thalassinos *et al* method can be greatly simplified through the use of the Amphitrite software library which allows fast calculation of calibration curves and CCS values.[35]

It is theorised that during ion mobility separation, high concentrations of ions will lead to densely charged ion packets, especially for ions that have a similar mobility. The high density of ions leads to an electrostatic repulsive force exerted from the centre of the ion cloud, causing expansion of the ion packet, in what is known as the *'space charge effect'* or *'coulombic expansion'*.[36] This leads to broadening of the arrival time distribution and is dependent on a variety of factors including the density of the mass and charge of the ions and the density of the ion packet. Some work has been done to use this effect to find unresolved conformers within wide ATDs.[37] However, this effect poses a particular problem for TWIMS CCS calibration as, if the concentration of the calibrants is not taken into account, inaccurate calibration may occur due to the broadening of arrival time distributions.

In this study we investigate the effect of calibrant concentration on the CCS calculation for the protein α-amylase, showing that high calibrant concentration causes a broadening of the ATD and a shift in the peak top, leading to higher calculated CCS values.

Methods

Sample preparation: Three calibrants were used: avidin (Thermo Fisher, Loughborough, UK), β-Lactoglobulin (Sigma, Gillingham, UK) and bovine serum albumin (Sigma). The protein of unknown CCS was α-amylase from *Bacillus licheniformis* (Sigma). Proteins were buffer exchanged using Amicon ultra centrifugal filtration units (Merck Millipore, Watford, UK) into 200 mM ammonium acetate solution. Buffer exchanged calibrant proteins were prepared to 5 μM, 10 μM, 20 μM and 30 μM (β-Lactoglobulin was assumed to be monomeric), and α-amylase was prepared to 10 μM. For all samples the concentration was calculated by both Qubit Protein Assay Kit (Thermo Fisher) and Nanodrop 2000 (Thermo Fisher) to ensure accuracy.

Data collection: Proteins were sprayed using nESI from gold-coated capillaries prepared *in-house* using a Flaming Brown P97 needle puller (Sutter Instruments Co, Novato, CA, USA) and a Q150R S sputter coater (Quorum Technologies, Lewes, UK). Data was collected on a Synapt G1 QToF mass spectrometer (Waters, Wilmslow, UK) using the following parameters: capillary volatage 1.2 kV, source voltage 40 V, extraction cone voltage 1 V, trap collision energy 8 eV, transfer collision energy 6 eV, bias voltage 16 V, IMS wave velocity 250 ms^{-1}, IMS wave height 8 V. For greater detail, please see Table S1 (supporting information). Data was collected on 3 separate days and samples were prepared on the day of data collection.

Data analysis: Data were processed using MassLynx v4.1 software (Waters) and arrival time distributions were extracted manually at the full-width at half maximum (FWHM) intensity using Driftscope (v2.0) (Waters). CCS calculations were performed manually using the method described by *Thalassinos et al.*[34] Briefly, the corrected drift time, *t(d)''*, is plotted against the

mass corrected CCS, *Ω'*, and creates a power-fit trend curve. For CCS calibration curves see Figures S1 – 3 (supporting information). $IWSD_{ATD}$ was calculated using the following equation:

$$IWSD_{ATD} = \sqrt{\frac{\sum_{i=1}^{n} I_i \left(t_i - \frac{\sum_{i=1}^{n} I_i t_i}{\sum_{i=1}^{n} I_i} \right)^2}{\sum_{i=1}^{n} I_i}}$$

where I is the intensity in each time arrival, t is the arrival time and n is the number of data points in the arrival time axis. Significance was calculated using a two tail T-test, based on the mean and standard deviation between 5 and 30 μM.

Results

Triplicate IMS spectra were collected for the full spectrum of three CCS calibrant proteins at increasing concentrations. The arrival time distributions for all proteins were observed to broaden and shift towards higher mobility species (Figure 1), showing that concentration does affect protein mobility in the gas phase. During CCS calibration the drift-time for the most intense point of the arrival time distribution, the peak top, is converted to a mass-corrected drift-time: *t(d)''*. All charge states from all calibrants show a significant decrease in *t(d)''* as the protein concentration increases from 5 μM to 30 μM (Figures 2A-D, Table) indicating that calibrant concentration has a direct effect on the TWIMS arrival time distribution. The samples sprayed at 5 μM show the lowest deviation of *t(d)''* across the charge states, suggesting that it may be the preferable concentration at which to run calibrants.

The peak broadening at increasing protein concentrations can be observed by using a complementary statistic known as intensity weighted standard deviation of the ATD ($IWSD_{ATD}$), which has been used as an empirical method of comparing collision induced unfolding fingerprints[38] (Figures 2E-H, Table 2). The difference in $IWSD_{ATD}$ is statistically significant between 5 μM and 30 μM in 50 % of cases, and generally follows the trend of an increase in $IWSD_{ATD}$ with increasing concentration. The Avidin +15 charge state shows a significant drop in $IWSD_{ATD}$; however, it is not clear why this is occurs. Some cases, such as the Avidin +18 charge state, display highly variable $IWSD_{ATD}$ values; however, this results from the high signal to noise ratio in some data sets due to a lowly populated charge state.

Being able to identify which calibrants are more likely to be affected by coulombic expansion would prove useful, and it might be expected that molecules which have a higher charge density per mass unit will experience a greater coulombic expansion effect, *i.e.* increase in concentration effect; however, this is not the case. The coulombic effect is dependent on the charge on the surface of the ion packet, which will relate to ion charge, ion cloud density and mobility affects.[39] This complexity may help explain why the +15 charge state of Avidin appears to show the reverse trend of decreasing $IWSD_{ATD}$ with increasing concentration.

To show that concentration of calibrants affects CCS calculation, the different calibrant conditions were used to calculate the CCS of the +13 to +15 charge states of 10 μM α-amylase.

The observed drop in the extracted *t(d)''* of calibrant ions would mean that the CCS calibrant values are effectively lower, leading to an increase in the calculated CCS value. As predicted, increased calibrant concentration led to an increase in the calculated CCS values across all charge states (Figure 3). The CCS values for the +13 to +15 charge states ranged from approximately 3300 to 3620 $Å^2$ (Table 3), with an increase of approximately 150 – 200 $Å^2$ for each charge state from 5 to 30 μM. This difference was statistically significant for the +14 and +15 charge states, but not for the +13.

Discussion and Conclusion

Increasing the concentration of protein calibrants has an effect on both the peak top and the peak width of ATDs due to the coulombic expansion effect. The increased density of the ion cloud appears to cause ions to expand in a leading front during TWIMS separation, explaining both the decreased arrival time and the peak broadening observed. It is difficult to recommend a standard concentration for CCS calibrants as the strength of the coulombic effect relies on a complex series of factors including, but not limited to, mass, charge and charge density of the ion packet.[39] The largest resource for CCS calibrants for proteins, the Bush calibrant library[40], does not report the protein concentration at which the CCS were calculated from DTIMS, nor do earlier published results from other groups;[7,41] however, the Ruotolo *et al* method recommends a concentration of 10 μM.[32] A concentration of 5 μM appears to have the lowest variation of t(d)'' for calibrants, and so may be recommendable as a standard concentration to use. Lower concentrations may obviously be used; however, sensitivity and the acquisition time should be taken into account. Quadrupole isolation of the calibrant charge states should also reduce the ion packet density and so alleviate concentration effects. Another option is to make use of the programmable dynamic range enhancement (pDRE) lens in Synapt models, which allows splitting or attenuation of the ion packet as it transfers from the quadrupole to the trapping cell, and it can be used to reduce the number of ions introduced into the IM cell. Using the quadrupole and pDRE lens to attenuate the ion packet until the peak top value of the arrival time distribution does not change may be easier and less time consuming to implement than altering the protein concentration. This study shows that the concentration of CCS calibrants should be considered during TWIMS studies as it may cause artefactual inflation of calculated CCS values. Proper reporting of ion preparation, as recommended in a recent paper by Gabelica, *et al*,[6] and following previously stated recommendations to alleviate coulombic expansion may help give more robust calculated TWIMS CCS values.

References

1. Macha SF, Limbach PA. Matrix-assisted laser desorption/ionization (MALDI) mass spectrometry of polymers. *Curr Opin Solid State Mater Sci*. 2002;6(3):213-220. doi:10.1016/S1359-0286(02)00036-0

2. Yamashita M, Fenn JB. Electrospray ion source. Another variation on the free-jet theme. *J Phys Chem*. 1984;88(20):4451-4459. doi:10.1021/j150664a002

3. Fenn JB. Electrospray ionization mass spectrometry: How it all began. *J Biomol Tech*. 2002;13(3):101-118. doi:10.1126/science.2675315

4. Robinson CV, Chung EW, Kragelund BB, et al. Probing the nature of noncovalent interactions by mass spectrometry. A study of protein-CoA ligand binding and assembly. *J Am Chem Soc*. 1996;118(36):8646-8653. doi:10.1021/ja960211x

5. Miranker A, Robinson CV, Radford SE, Aplin RT, Dobson CM. Detection of transient protein folding populations by mass spectrometry. *Science (80-)*. 1993;262(5135):896-900. doi:10.1126/science.8235611

6. Gabelica V, Shvartsburg AA, Afonso C, et al. Recommendations for reporting ion mobility Mass Spectrometry measurements. *Mass Spectrom Rev*. February 2019. doi:10.1002/mas.21585

7. Shelimov KB, Clemmer DE, Hudgins RR, Jarrold MF. Protein structure in Vacuo: Gas-phase conformations of BPTI and cytochrome c. *J Am Chem Soc*. 1997;119(9):2240-2248. doi:10.1021/ja9619059

8. Wojnowska M, Yan J, Sivalingam GN, et al. Autophosphorylation activity of a soluble hexameric histidine kinase correlates with the shift in protein conformational equilibrium. *Chem Biol*. 2013;20(11):1411-1420. doi:10.1016/j.chembiol.2013.09.008

9. Dickinson ER, Jurneczko E, Pacholarz KJ, et al. Insights into the Conformations of Three Structurally Diverse Proteins: Cytochrome c, p53, and MDM2, Provided by Variable-Temperature Ion Mobility Mass Spectrometry. *Anal Chem*. 2015;87(6):3231-3238. doi:10.1021/ac503720v

10. Nyon MP, Prentice T, Day J, et al. An integrative approach combining ion mobility mass spectrometry, X-ray crystallography, and nuclear magnetic resonance spectroscopy to study the conformational dynamics of α1-antitrypsin upon ligand binding. *Protein Sci*. 2015;24(8):1301-1312. doi:10.1002/pro.2706

11. Landreh M, Marklund EG, Uzdavinys P, et al. Integrating mass spectrometry with MD simulations reveals the role of lipids in Na+/H+ antiporters. *Nat Commun*. 2017;8:13993. doi:10.1038/ncomms13993

12. Hyung SJ, Robinson CV, Ruotolo BT. Gas-Phase Unfolding and Disassembly Reveals Stability Differences in Ligand-Bound Multiprotein Complexes. *Chem Biol*. 2009;16(4):382-390. doi:10.1016/j.chembiol.2009.02.008

13. Benesch JLP. Collisional Activation of Protein Complexes: Picking Up the Pieces. *J Am Soc Mass Spectrom*. 2009;20(3):341-348. doi:10.1016/j.jasms.2008.11.014

14. Bernstein SL, Dupuis NF, Lazo ND, et al. Amyloid-β 2 protein oligomerization and the importance of tetramers and dodecamers in the aetiology of Alzheimer's disease.

Nat Chem. 2009;1(4):326-331. doi:10.1038/nchem.247

15. Bleiholder C, Wyttenbach T, Bowers MT. A novel projection approximation algorithm for the fast and accurate computation of molecular collision cross sections (I). Method. *Int J Mass Spectrom*. 2011;308(1):1-10. doi:10.1016/j.ijms.2011.06.014

16. Viehland LA, Mason EA. Gaseous ion mobility and diffusion in electric fields of arbitrary strength. *Ann Phys (N Y)*. 1978;110(2):287-328. doi:10.1016/0003-4916(78)90034-9

17. Creaser CS, Griffiths JMR, Bramwell CJ, Noreen S, Hill CA, Thomas CLP. Ion mobility spectrometry: A review. Part 1. Structural analysis by mobility measurement. *Analyst*. 2004;129(11):984-994. doi:10.1039/b404531a

18. Giles K, Pringle SD, Worthington KR, Little D, Wildgoose JL, Bateman RH. Applications of a travelling wave-based radio-frequency-only stacked ring ion guide. *Rapid Commun Mass Spectrom*. 2004;18(20):2401-2414. doi:10.1002/rcm.1641

19. Giles K, Williams JP, Campuzano I. Enhancements in travelling wave ion mobility resolution. *Rapid Commun Mass Spectrom*. 2011;25(11):1559-1566. doi:10.1002/rcm.5013

20. Pringle SD, Giles K, Wildgoose JL, et al. An investigation of the mobility separation of some peptide and protein ions using a new hybrid quadrupole/travelling wave IMS/oa-ToF instrument. *Int J Mass Spectrom*. 2007;261(1):1-12. doi:10.1016/j.ijms.2006.07.021

21. Giles K, Wildgoose JL, Langridge DJ, Campuzano I. A method for direct measurement of ion mobilities using a travelling wave ion guide. *Int J Mass Spectrom*. 2010;298(1-3):10-16. doi:10.1016/j.ijms.2009.10.008

22. Mortensen DN, Susa AC, Williams ER. Collisional Cross-Sections with T-Wave Ion Mobility Spectrometry without Experimental Calibration. *J Am Soc Mass Spectrom*. 2017;28(7):1282-1292. doi:10.1007/s13361-017-1669-0

23. Bush MF, Hall Z, Giles K, Hoyes J, Robinson CV, Ruotolo BT. Collision cross sections of proteins and their complexes: A calibration framework and database for gas-phase structural biology. *Anal Chem*. 2010;82(22):9557-9565. doi:10.1021/ac1022953

24. Valentine SJ, Counterman AE, Clemmer DE. A database of 660 peptide ion cross sections: use of intrinsic size parameters for bona fide predictions of cross sections. *J Am Soc Mass Spectrom*. 1999;10(11):1188-1211. doi:10.1016/S1044-0305(99)00079-3

25. Haler JRN, Kune C, Massonnet P, et al. Comprehensive Ion Mobility Calibration: Poly(ethylene oxide) Polymer Calibrants and General Strategies. *Anal Chem*. 2017;89(22):12076-12086. doi:10.1021/acs.analchem.7b02564

26. Duez Q, Chirot F, Liénard R, et al. Polymers for Traveling Wave Ion Mobility Spectrometry Calibration. *J Am Soc Mass Spectrom*. 2017;28(11):2483-2491. doi:10.1007/s13361-017-1762-4

27. Campuzano I, Bush MF, Robinson CV, et al. Structural characterization of drug-like compounds by ion mobility mass spectrometry: Comparison of theoretical and

experimentally derived nitrogen collision cross sections. *Anal Chem*. 2012;84(2):1026-1033. doi:10.1021/ac202625t

28. Salbo R, Bush MF, Naver H, et al. Traveling-wave ion mobility mass spectrometry of protein complexes: Accurate calibrated collision cross-sections of human insulin oligomers. *Rapid Commun Mass Spectrom*. 2012;26(10):1181-1193. doi:10.1002/rcm.6211

29. Bush MF, Campuzano IDG, Robinson CV. Ion mobility mass spectrometry of peptide ions: Effects of drift gas and calibration strategies. *Anal Chem*. 2012;84(16):7124-7130. doi:10.1021/ac3014498

30. May JC, Morris CB, McLean JA. Ion Mobility Collision Cross Section Compendium. *Anal Chem*. 2017;89(2):1032-1044. doi:10.1021/acs.analchem.6b04905

31. Allen SJ, Schwartz AM, Bush MF. Effects of Polarity on the Structures and Charge States of Native-Like Proteins and Protein Complexes in the Gas Phase. *Anal Chem*. 2013;85:46. doi:10.1021/ac403139d

32. Ruotolo BT, Benesch JLP, Sandercock AM, Hyung S-J, Robinson CV. Ion mobility–mass spectrometry analysis of large protein complexes. *Nat Protoc*. 2008;3(7):1139-1152. doi:10.1038/nprot.2008.78

33. Smith D, Knapman T, Campuzano I, et al. Deciphering drift time measurements from travelling wave ion mobility spectrometry-mass spectrometry studies. *Eur J Mass Spectrom*. 2009;15(5):113. doi:10.1255/ejms.947

34. Thalassinos K, Grabenauer M, Slade SE, et al. Characterization of Phosphorylated Peptides Using Traveling Wave-Based and Drift Cell Ion Mobility Mass Spectrometry Characterization of Phosphorylated Peptides Using Traveling Wave-Based and Drift Cell Ion Mobility Mass Spectrometry. *Anal Chem*. 2009;81(1):248-154. doi:10.1021/ac801916h

35. Sivalingam GN, Yan J, Sahota H, Thalassinos K. Amphitrite: A program for processing travelling wave ion mobility mass spectrometry data. *Int J Mass Spectrom*. 2013;345-347:54-62. doi:10.1016/j.ijms.2012.09.005

36. Richardson K, Langridge D, Giles K. Fundamentals of travelling wave ion mobility revisited: I. Smoothly moving waves. *Int J Mass Spectrom*. 2018;428:71-80. doi:10.1016/j.ijms.2018.03.007

37. Kune C, Far J, De Pauw E. Accurate drift time determination by traveling wave ion mobility spectrometry: The concept of the diffusion calibration. *Anal Chem*. 2016;88(23):11639-11646. doi:10.1021/acs.analchem.6b03215

38. Sivalingam GN, Cryar A, Williams MA, Gooptu B, Thalassinos K. Deconvolution of ion mobility mass spectrometry arrival time distributions using a genetic algorithm approach: Application to α1-antitrypsin peptide binding. *Int J Mass Spectrom*. 2018;426:29-37. doi:10.1016/j.ijms.2018.01.008

39. Tolmachev AV, Clowers BH, Belov ME, Smith RD. Coulombic effects in ion mobility spectrometry. *Anal Chem*. 2009;81(12):4778-4787. doi:10.1021/ac900329x

40. Bush MF, Hall Z, Giles K, Hoyes J, Robinson CV, Ruotolo BT. Collision cross

sections of proteins and their complexes: A calibration framework and database for gas-phase structural biology. *Anal Chem*. 2010;82(22):9557-9565. doi:10.1021/ac1022953

41. Valentine SJ, Anderson JG, Ellington AD, Clemmer DE. Disulfide-Intact and -Reduced Lysozyme in the Gas Phase: Conformations and Pathways of Folding and Unfolding. *J Phys Chem B*. 2002;101(19):3891-3900. doi:10.1021/jp970217o

Table 1 Mean t(d)'' peak top values for CCS calibrant proteins at different concentrations, to 3 s.f. with standard deviation to 3 s.f, * denotes values averaged from duplicates not triplicates.

Protein	z	t(d)''			
		5 µM	10 µM	20 µM	30 µM
Avidin	15	*4.84 ± 4.85E-8	3.52 ± 0.275	3.40 ± 0.180	3.28 ± 0.104
	16	2.75 ± 0.208	2.09 ± 0.275	1.97 ± 3.10E-8	2.03 ± 0.275
	17	1.91 ± 0.104	1.37 ± 0.104	1.07 ± 6.00E-8	1.19 ± 0.208
	18	1.44 ± 1.44E-8	1.08 ± 0.180	1.02 ± 0.104	1.14 ± 0.104
BSA	14	8.49 ± 0.208	8.31 ± 0.208	7.77 ± 0.375	7.59 ± 0.208
	15	6.27 ± 0.180	5.85 ± 0.416	5.01 ± 0.360	4.83 ± 3.80E-8
	16	4.84 ± 0.312	4.48 ± 0.360	3.82 ± 0.275	3.46 ± 0.104
	17	4.30 ± 0.312	3.88 ± 0.275	3.16 ± 0.375	2.92 ± 0.104
βLac (1mer)	7	3.92 ± 0.104	3.68 ± 0.208	3.44 ± 2.20E-8	3.02 ± 0.275
	8	2.58 ± 0.312	2.37 ± 0.180	2.25 ± 0.208	1.89 ± 0.208
	9	2.20 ± 0.312	1.90 ± 0.275	1.78 ± 0.375	1.66 ± 0.105
βLac (2mer)	11	5.70 ± 0.105	5.64 ± 0.275	5.22 ± 0.312	4.56 ± 0.375
	12	4.33 ± 0.180	3.91 ± 0.275	3.55 ± 0.104	3.07 ± 0.312
	13	3.61 ±0.180	3.31 ± 0.375	2.83 ± 0.104	2.35 ± 0.312

Table 2: Mean $IWSD_{ATD}$ values for CCS calibrant proteins at different concentrations, to 3 s.f. with standard deviation to 3 s.f, * denotes values averaged from duplicates not triplicates.

Protein	z	IWSD			
		5 µM	10 µM	20 µM	30 µM
Avidin	15	*1.02 ± 5.85E-02	0.920 ± 1.30E-01	0.920 ± 7.67E-02	0.892 ± 1.26E-01
	16	0.596 ± 8.76E-03	0.652 ± 2.67E-02	0.694 ± 3.10E-02	0.670 ± 5.61E-02
	17	0.440 ± 4.34E-03	0.501 ± 2.71E-02	0.538 ± 1.03E-02	0.522 ± 3.84E-02
	18	0.485 ± 1.00E-01	0.817 ±3.61E-01	0.871 ± 9.18E-02	1.01 ± 3.97E-01
BSA	14	1.12 ± 8.21E-02	1.27 ± 1.23E-01	1.354 ± 1.24E-01	1.414 ± 3.44E-02
	15	0.716 ± 2.27E-02	0.772 ± 4.85E-02	0.839 ±3.17E-02	0.849 ± 2.63E-02
	16	0.530 ± 9.65E-03	0.575 ± 4.05E-02	0.672 ± 5.72E-02	0.713 ± 3.42E-02
	17	0.611 ± 9.13E-02	0.516 ± 2.12E-02	0.572 ± 1.41E-02	0.602 ±1.13E-02
βLac (1mer)	7	0.500 ± 4.11E-02	0.584 ± 5.37E-02	0.636 ± 3.48E-02	0.678 ± 2.74E-02
	8	0.462 ± 2.86E-02	0.487 ± 2.21E-02	0.506 ± 2.63E-02	0.546 ± 4.52E-02
	9	0.477 ± 3.49E-02	0.489 ± 1.37E-02	0.539 ± 5.73E-02	0.636 ± 1.10E-01
βLac (2mer)	11	0.751 ± 5.38E-02	0.837 ± 1.22E-01	0.886 ± 5.14E-02	0.898 ± 1.03E-01
	12	0.552 ±1.29E-02	0.624 ± 2.60E-02	0.695 ±3.72E-02	0.776 ± 3.67E-02
	13	0.385 ± 2.26E-02	0.453 ± 6.91E-02	0.515 ± 5.60E-02	0.547 ± 3.86E-02

Table 3: Experimentally calculated CCS values for α-amylase at different calibrant concentration, using the Thalassinos method.

Calibrant Concentration	Calculated Collision Cross-Section (Å^2)		
	+13	**+14**	**+15**
5 µM	3371 ± 82.2	3314 ± 53.6	3407 ± 74.1
10 µM	3394 ± 81.3	3388 ± 47.4	3506 ± 54.2
20 µM	3453 ± 72.7	3450 ± 38.5	3572 ± 46.9
30 µM	3547 ± 101	3510 ± 46.3	3619 ± 62.3

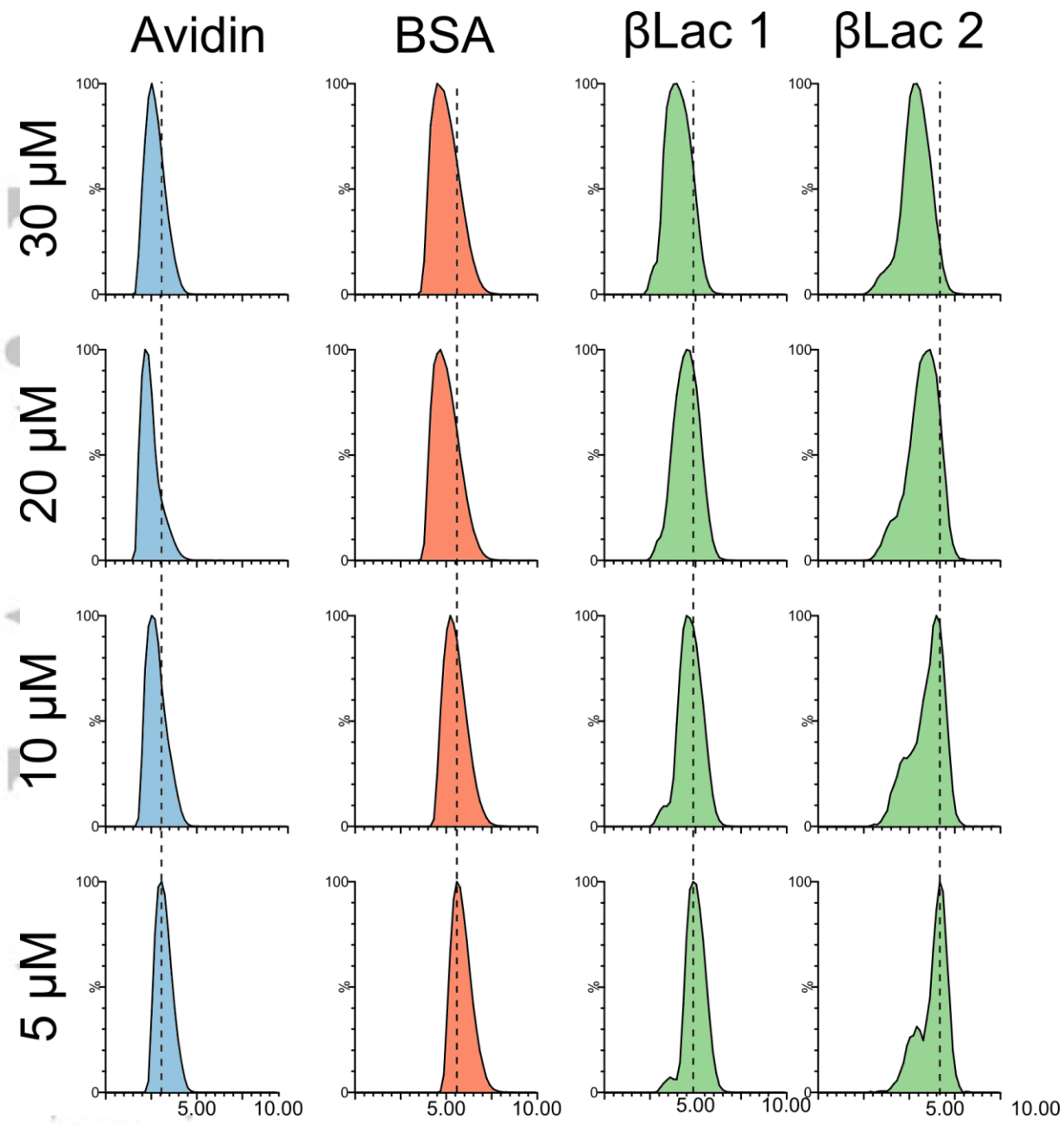

Figure 1 Arrival time distributions at 5, 10, 20 and 30 μM for A) Avidin +17 B) BSA +16 C) βLac +7 (monomeric) D) βLac +11 (dimeric), collected on a single day. The dotted line for each shows the peak top for the ATD at 5 μM, showing a shift to lower arrival times and distribution broadening as concentration increases.

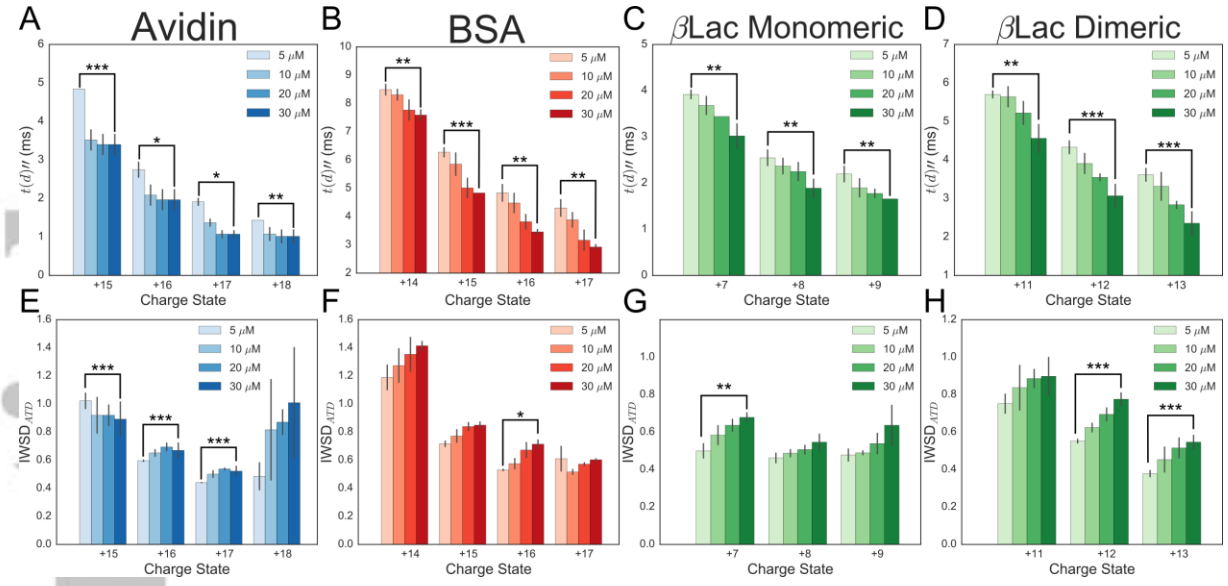

Figure 2 Average mass corrected drift time peak top values (t(d)'') values for Bush library calibrants at different concentrations, with standard deviation error bars (A – D). For some charge states error bars are too small to be seen. A) Avidin B) BSA C) βLac monomeric D) βLac dimeric. Average intensity weighted standard deviation of arrival time distributions (IWSDATD) values for Bush library calibrants at different concentrations, with standard deviation error bars (E – H). E) Avidin F) BSA G) βLac monomeric H) βLac dimeric. Significance threshold: * = $p < 0.05$, ** = $p < 0.005$, *** = $p < 0.0005$

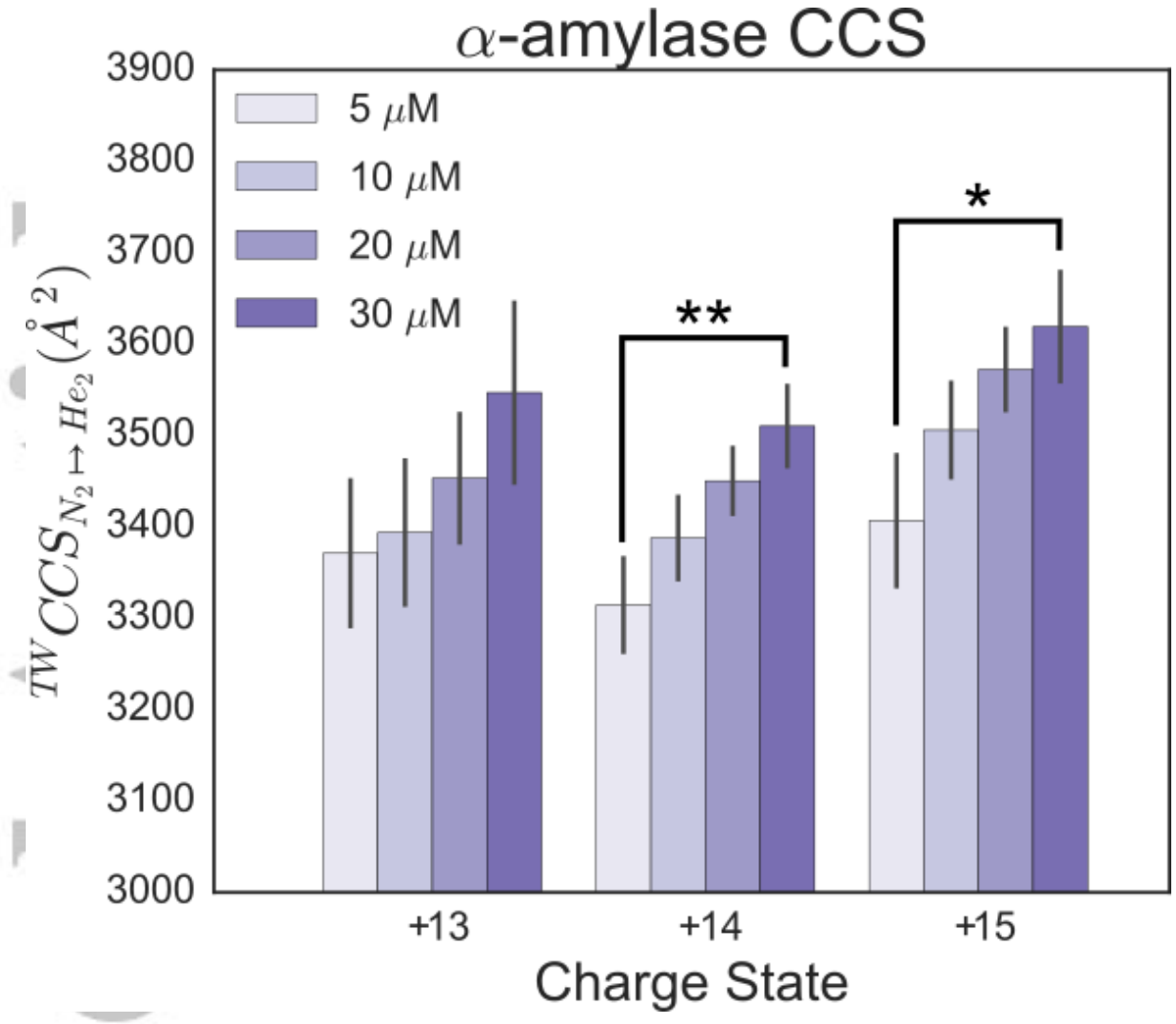

Figure 3 Calculated CCS values for 10 μM α-amylase at different concentrations of CCS calibrants. Significance threshold: * = $p < 0.05$, ** = $p < 0.005$